ISBN: 978-3-95450-196-0 doi:10.18429/JACoW-ECRIS2018-TUP13

CHARACTERIZATION OF ECR PLASMA BY MEANS OF RADIAL AND AXIAL X-RAY DIAGNOSTICS

R. Miracoli†, ESS Bilbao, Poligono Ugaldeguren III,Pol. A, 7B. 48170 Zamudio, Spain
G. Castro, L. Celona, S. Gammino, D. Mascali, M. Mazzaglia, E. Naselli[1], G. Torrisi
INFN-LNS,Via S. Sofia 62, 95123, Catania, Italy
[1] Universitá degli studi di Catania, Dipartimento di Fisica e Astronomia,
Via S. Sofia 64, 95123, Catania, Italy

Abstract

This work presents the X -ray characterization of the plasma generated in a simple mirror axis symmetric trap as a function of the magnetic field profile. A Si-Pin detec-tor has been used to characterize warm electron populati-on in axial and radial directions at two different operating frequencies: 4.1 GHz and 6.8 GHz. Moreover, the hot electrons emitted in axial direction has been measured by means of a HyperPure Germanium (HpGe) detector. Results show that X-ray emission is not homogenous and its homogeneity and temperature depends strongly on the magnetic field profile.

INTRODUCTION

The electron cyclotron resonance ion sources (ECRIS) are mainly used to produce highly charged ions currents for accelerators, nuclear physics research and industrial applications. In recent years many studies have been made in order to understand better the wave-to-plasma interactions that produce plasma instability [1], in particu-lar about the non-linear response of electron heating to pumping wave frequency and anisotropy in plasma densi-ty and electron energy distribution function [2,3]. It is observed that B_{min} value (the minimum value in the mid-plane of the plasma chamber), changes the gradient (de-scribed here in terms of B_{min}/B_{ECR} ratio) of the magnetic field close to ECR surface. The moderate gradient, ob-tained for higher B_{min}, increases the ECR heating effi-ciency and the electron temperature in the plasma. More-over, it is noted that in a moderate gradient regime the plasmas become unstable and can generate intense emis-sions of fluxes of bremsstrahlung and microwaves. In this paper we wanted to show the characterization of the Flexible Plasma Trap (FPT) through measurements of x-rays spectra, acquired by HyperPure Germanium (HpGe) and Si-Pin detectors. X-rays were recorded in both the radial and axial directions for different magnetic field profiles and frequency heating.

EXPERIMENTAL SET-UP

FPT is a test bench for plasma diagnostics and develop-ment of new sources, operating at INFN-LNS [4]. Three solenoids generate different magnetic profiles (off-resonance, simple mirror and magnetic beach configuration) and allow to tune the magnetic field value as a function of the frequency. FPT has three different microwave sys-tems, one parallel and two perpendicular respect to the plasma chamber. The axial injection operates from 4 to 7 GHz. The signal is generated by a Rohde & Schwarz generator, amplified by a TWT and sent to the FPT by WRD350 waveguides. The axial microwave line is com-posed by a directional coupler and an isolator to protect the TWT from the reflected power. The perpendicular microwave launcher can work at 14 GHz and allow oper-ating in double frequency (first and second frequency) mode [5]. The water-cooled copper plasma chamber is 260.1 mm length and its inner diameter is about 82 mm. A stainless-steel vacuum chamber is connected to the plas-ma chamber to host the vacuum system and the diagnostic tools. Figure 1 shows the schematic drawing of the FPT and the diagnostics.

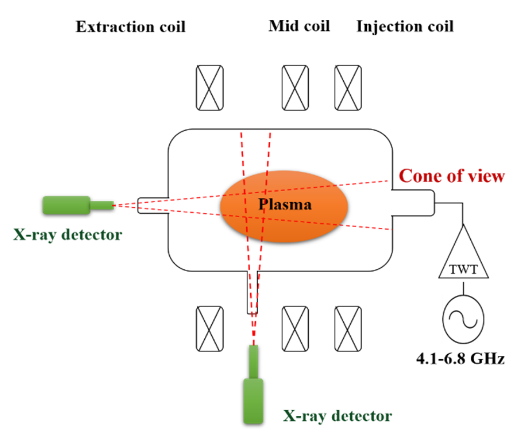

Figure 1: Schematic drawing of the FPT and of x-rays detectors used during the experimental campaign.

High energy X radiation was detected by a HpGe, lo-cated on the axial port of the vacuum chamber, the detec-tor was used for monitoring the x-rays generated by the high energy electrons, from inside the plasma or when they hit the vacuum vessel walls. The HpGe consists of a 15 mm thick, 20 cm^2 crystal protected by a 0.3 mm thick Be window. Its resolution at 122 keV is 0.61 keV. The detector is shielded with lead blocks of 2 cm thickness and ϕ= 1 mm to avoid detecting x-rays scattered from the environmental material. The HpGe detects the radiation

† rmiracoli@essbilbao.org

ISBN: 978-3-95450-196-0 doi:10.18429/JACoW-ECRIS2018-TUP13

that pass mostly through the collimator of the vacuum vessel.

In the second part of the investigation two Si-Pin detectors (XR-100CR, AMPTEK) were used, one placed on the axial port of the vacuum chamber and the other on the radial port of the plasma chamber. Their resolution at 5.9 keV are about 200 eV and the Be window has a thickness of 1 mm. Both detectors are used for monitoring the x-rays generated by electrons from a few keV to several tens of keV.

All raw data have been corrected for detector intrinsic efficiencies, which include the correction for the beryllium window, the Kapton foil for vacuum break, and the air attenuation. Once the correction is made it is possible to calculate the spectral temperature, T_e, by fitting a straight line to experimental data in a semilogarithmic plot over a selected range of energy [6]. T_e can be obtained from the inverse of the line slope and is used to determine an estimate for the mean energy of the hot electrons. The x-rays are collimated by a lead cylinder with a hole of ϕ =1 mm and 6 cm in length.

EXPERIMENTAL RESULTS

In the first part of the experiment we used the HPGe detector, to investigate how the variation of the magnetic field gradient can affect the rate of axial bremsstrahlung and the electron distribution of energy. For the two-heating frequencies: 4.1 and 6.83 GHz we have fixed the current of the injection and extraction coils and have set the current of the mid coil to shift the B_{min}/B_{ECR} ratio from 0.56 to 1.02. Figure 2 shows some of the magnetic configurations that we used at 6.8 GHz. All data were recorded at a power level of 80 W and typical operating pressures in vacuum chamber are about $8 \cdot 10^{-5}\,mbar$.

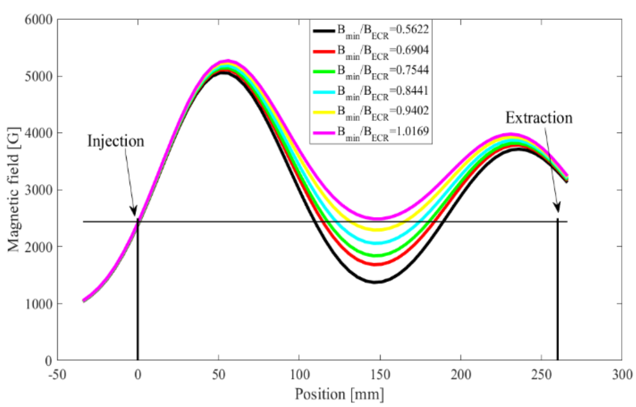

Figure 2: Simple mirror configurations used at 6.8 GHz as heating frequency. The injection and extraction coil currents have been fixed at 440 and 441 A respectively, while the mid coil has been changed from -88 A to 60 A. The change in mid coil current allowed to modify the B_{min}/B_{ECR} ratio along the plasma chamber axis from 0.56 to 1.02. ($B_{ECR} = 2440\,G$ at 6.8 GHz).

The trend of the rate (counts/s) detected by HPGe, at 6.8 GHz, is shown in Fig. 3, where two regions can be identified: for value B_{min}/B_{ECR} less than ~0.8 the x-ray emitted is negligible while for B_{min}/B_{ECR} higher than ~0.8 the rate increases suddenly. At 4.1 GHz, instead, the magnitude of bremsstrahlung changes considerably for $B_{min}/B_{ECR} > 1$. For the first heating frequency value we have calculated the spectral temperature. The energy range where we did the linear fit to semilogarithmic bremsstrahlung spectra was about 50-75 keV for $B_{min}/B_{ECR} > 0.8$, and about 10-16 keV for $B_{min}/B_{ECR} < 0.8$. It was necessary to modify the energy range to calculate the electron temperature because the shape and the intensity of x-ray spectra are completely different in the two regions. In fact, a sharp increase of T_e is illustrated in Fig. 4, where the temperature shifts from 3 to 15 keV.

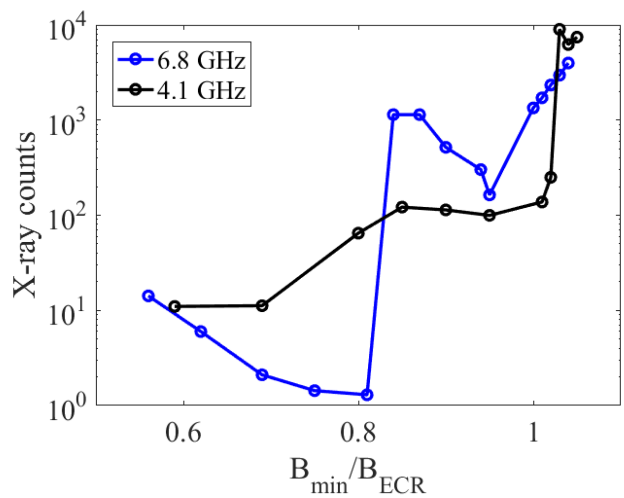

Figure 3:X-ray emission rate versus different simple mirror configurations. For both the frequencies, the pressure and the absorbed power are $8 \cdot 10^{-5}\,mbar$ and 80 W, respectively.

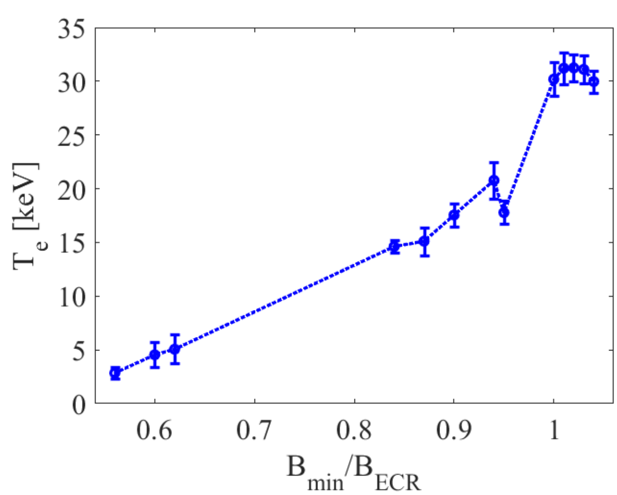

Figure 4: The dependence of T_e versus different simple mirror configurations.

The measurements continued by using the Si-Pin detectors to record radial and axial x-rays spectra, at a power level of 80 W and pressures of about $8 \cdot 10^{-5}\,mbar$, as in the first part of the experiment. In Fig. 5 there is a direct comparison between the x-rays spectra measured at both

ISBN: 978-3-95450-196-0 doi:10.18429/JACoW-ECRIS2018-TUP13

positions. Here again we wanted to investigate the effects on bremsstrahlung spectra by changing the magnetic field profile. The Bremsstrahlung of the axial x-rays spectrum are much greater than those radial, because the geometric efficiency for the two geometric systems is different. The radial spectrum has only the k_α of Ar (2.96 keV), k_α and k_β of Cu (8.05 keV and 8.9 keV respectively). Instead, in the axial spectrum we can see also k_α of Cr (5.41 keV) and Fe (6.40 keV), due to several scattering coming out from the stainless-steel diagnostic box. The peaks of Ar k_α are less affected from the bremsstrahlung produced outside the plasma chamber and the change in their intensity can be correlated mainly to two different geometric efficiencies (named solid angle and plasma volume).

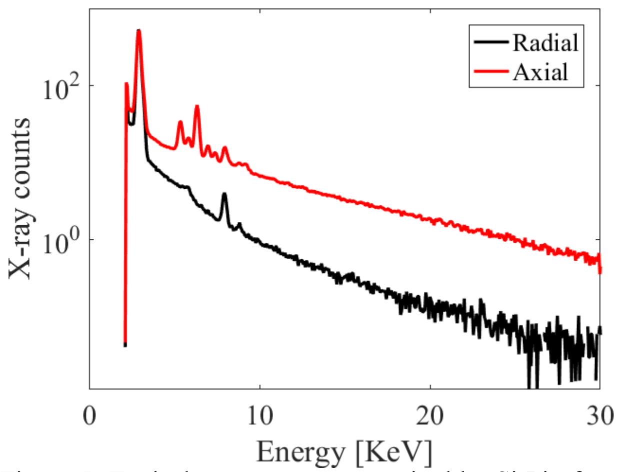

Figure 5: Typical x-rays spectra acquired by Si-Pin from axial and radial ports. Fluorescence lines of Ar and Cu are visible in both spectra. The pressure and the absorbed power are $8\cdot 10^{-5}$ mbar and 80 W, respectively.

Measurements of Ar k_α intensity and x-rays in both the radial and axial directions, were performed by Kato [7], in an ECR multicharged ions source by changing the microwave power and pressure, but not the magnetic profiles. In Fig. 6 there is the trend of the $k\alpha_{Rad}/k\alpha_{Axl}$, the ratio between the intensity of Ar k_α emitted in radial and axial directions, as a function of B_{min}/B_{ECR}. Axial k_α intensity is about 3-4 times larger than it is in the radial direction and changes slightly from the different magnetic profiles, where each peak has been calculated after having subtracted the bremsstrahlung counts.

Afterwards we used the $k\alpha_{Rad}/k\alpha_{Axl}$ ratio that includes information about the solid angle and plasma volume to normalize the spectra. In Fig. 7, there is the trend of the bremsstrahlung rate detected by Si-Pin. As in the previous measurements shown in Fig. 3, the detectors in both directions reveal few counts for $B_{min}/B_{ECR} < 0.8$ but the rate suddenly increases for $B_{min}/B_{ECR} > 0.8$. In each emission region the axial rate is higher than the radial one. Figure 8 compares the spectral temperature obtained from the axial and radial ports in function of the magnetic profile. The energy range used to do the linear fit was about 10-14 keV for all the spectra. As in the Figs. 3 and 4 two regions can be identified: one with $B_{min}/B_{ECR} < 0.8$ characterized by few x-ray counts and low temperature (< 5 keV), the other for $B_{min}/B_{ECR} >$ 0.8 where plasmas generate strong bremsstrahlung emission and very energetic electrons.

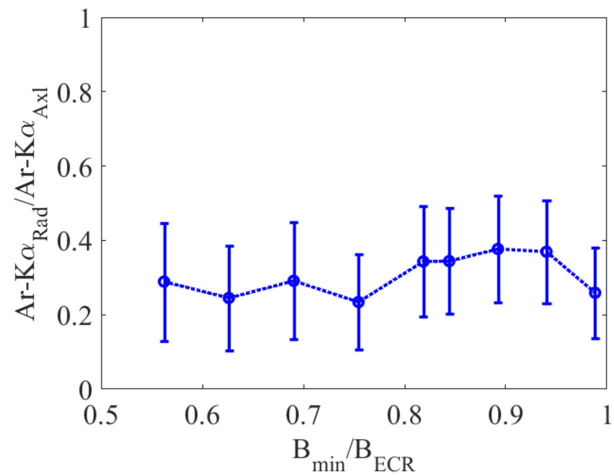

Figure 6: Trend of $k\alpha_{Rad}/k\alpha_{Axl}$ ratio versus different simple mirror configurations.

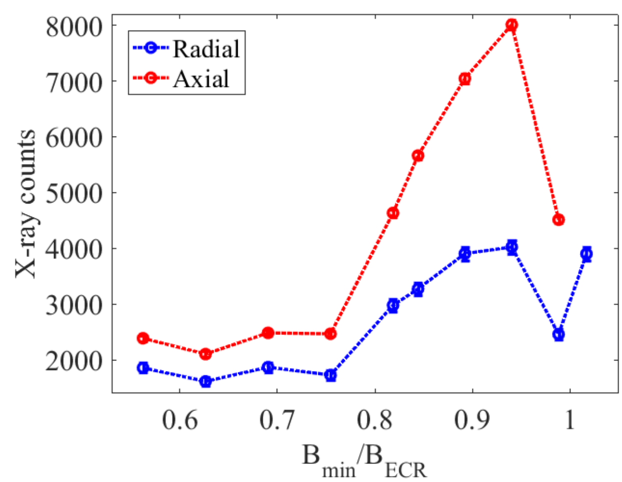

Figure 7: X-ray emission rate acquired from axial and radial ports versus different simple mirror configurations.

It has been observed in previous work [8,9], that the decrease of B_{min} improves the electron confinement, and so the source performance, but when B_{min} is increased ($B_{min}/B_{ECR} > 0.8$) non linear effects take place. The magnetic field gradient becomes lower in a large part of the ECR surface and the electrons gain more energy for a single crossing of the resonance. These hot electrons escape from the magnetic confinement and raise the rate of bremsstrahlung emission.

Moreover, the trends of the temperature measured in both the Si-Pin, make aware that for $B_{min}/B_{ECR} < 0.8$ the electron temperature are almost identical in axial and radial directions, and only in the second region, for $B_{min}/B_{ECR} > 0.8$, the axial T_e increases faster than radial T_e. The trend of the axial T_e obtained with the Si-Pin is similar to the one obtained from HPGe detector, in Fig. 4.

ISBN: 978-3-95450-196-0 doi:10.18429/JACoW-ECRIS2018-TUP13

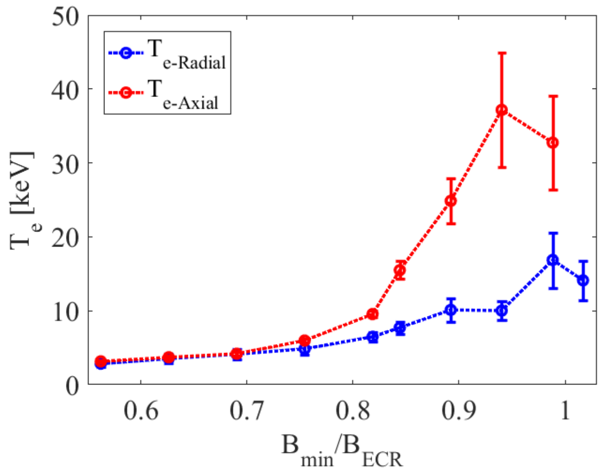

Figure 8: The dependence of T_e versus different simple mirror configurations.

CONCLUSIONS

A study of bremsstrahlung emission was carried out with the FPT at INFN-LNS. The experimental results demonstrate that the x-ray production and electron temperature depend on the magnetic configuration: when B_{min}/B_{ECR} ratio is ≈ 0.8 plasmas start to strong x-ray emission. Furthermore, while for B_{min}/B_{ECR} <0.8 X ray emission show isotropic characteristics, when critical ratio is overcome, radial spectral temperature is lower than axial spectral temperature. The observed critical value of B_{min}/B_{ECR} is compatible with the passage from strong gradient to moderate gradient ECR regime [10]. Moreover, several fingerprints show that above the critical value, cyclotron instability may play an important role as already observed by other authors [2]. A dedicated paper will investigate the cyclotron instability emission revealed above the critical value of B_{min}/B_{ECR}. Further experimental measurements are also planned to characterize better the physic process that lead to the strong plasmas instabilities, with the aim to optimize the design of the future ions sources. FPT represents the better device to investigate the cyclotron instabilities since it allows the installation of different types of diagnostics, not only x-rays detectors, but also optical emission spectrometer [11], pin-hole camera and microwave interferometer [12,13] to characterize different range of the electron distribution function and the density of the whole plasma.

REFERENCES

[1] S. Gammino et al., "Considerations on the role of the magnetic field gradient in ECR ion sources and build-up of hot electron component", *Plasma Sources Sci. and Technol.*, vol. 18, p. 045016, 2016, https://doi.org/10.1088/0963-0252/18/4/045016

[2] O. Tarvainen et al., "*Beam current oscillations driven by cyclotron instabilities in a minimum-B electron cyclotron resonance ion source plasma*", *Plasma Sources Sci. and Technol.*, vol. 23, p. 025020, 2014, https://doi.org/10.1088/0963-0252/23/2/025020

[3] D. Mascali et al., "Electron cyclotron resonance ion source plasma characterization by X-ray spectroscopy and X-ray imaging", *Rev. Sci. Instrum*, vol. 87, p. 02A510, 2016, https://doi.org/10.1063/1.4939201

[4] S. Gammino et al., "The Flexible Plasma Trap (FPT) for the production of overdense plasmas", *JINST*, vol. 12, p. P07027, 2017 https://doi.org/10.1088/1748-0221/12/07/P07027

[5] G. Torrisi et al., "A new launching scheme for ECR plasma based on two-waveguides-array", *Microw. Opt. Technol. Lett.*, vol. 58, p. 2629, 2016, https://doi.org/10.1002/mop.30117

[6] D. Mascali et al., "X-ray spectroscopy of warm and hot electron components in the CAPRICE source plasma at EIS testbench at GSI", *Rev. Sci. Instrum.*, vol. 85, p. 02A956, 2014, https://doi.org/10.1063/1.4858115

[7] Y. Kato et al., Pulse height analysis using Si-Pin diode of x-ray irradiated from a 2.45 GHz electron cyclotron resonance multicharged ion source, Rev. Sci. Instrum., vol. 69,p. 1179, 1998, https://doi.org/10.1063/1.1148659

[8] J. Y. Benitez et al., Recent Bremsstrahlung Measurements from the Superconducting Electron Cyclotron Resonance Ion Source VENUS, in Proc. 22nd Int. Workshop on ECR Ion Sources (ECRIS'16), Busan, Korea, August 2016, MOCO04, pp. 23-29, https://doi.org/10.18429/JACoW-ECRIS2016-MOCO04

[9] J. Noland et al., "Studies of electron heating on a 6.4 GHz ECR ion source through measurement of diamagnetic current and plasma bremsstrahlung", *Plasma Sources Sci. and Technol.*, vol. 20, p. 035022, 2011, https://doi.org/10.1088/0963-0252/20/3/035022

[10] E. Canobbio, "Gyroresonant particle acceleration in a non-uniform magnetostatic field", *Nucl. Fusion*, vol. 9, p. 27, 1969, https://doi.org/10.1088/0029-5515/9/1/004

[11] G. Castro et al., Application of Optical Emission Spectroscopy to High Current Proton Sources, *in Proc. 8th Int. Particle Accelerator Conf.* (IPAC'17), Copenhagen, Denmark, May 2017, TUPIK020, pp. 1721-1723, https://doi.org/10.18429/JACoW-IPAC2017-TUPIK020

[12] D. Mascali et al., "The first measurement of plasma density in an ECRIS-like device by means of a frequency-sweep microwave interferometer", *Rev. Sci. Instrum.*, vol. 87, p. 095109, 2016, https://doi.org/10.1063/1.4963710

[13] Torrisi et al., "Microwave frequency sweep interferometer for plasma density measurements in ECR ion sources: Design and preliminary results", *Rev. Sci. Instrum.*, vol. 87, p. 02B909, 2016, https://doi.org/10.1063/1.4933025